Single-Molecule Study of Peptides with the Same Amino Acid Composition but Different Sequences by Using an Aerolysin Nanopore

Fangzhou Hu,[a] Borislav Angelov,[b] Shuang Li,[a] Na Li,[c] Xubo Lin,*[d] and Aihua Zou*[a]

Nanopores are original sensors employed for highly sensitive peptide/protein detection. Herein, we describe the use of an aerolysin nanopore to identify two similar model peptides, YEQYEQQDDDRQQQ (YEQ2Q3) and QDDDRQQQYEQYEQ (Q3YEQ2), with the same amino acid composition but different sequences. All-atom molecular dynamics (MD) simulations reveal that YEQ2Q3 possesses fewer hydrogen bonds and a more extended conformation than Q3YEQ2. These two peptides, which fold differently, exhibit obviously distinct mass-independent current blockades with characteristic dwell times when entering the aerolysin nanopore. Typically, at +60 mV,

the statistical dwell time of 0.630 ± 0.018 ms for peptide Q3YEQ2 is four times longer than the value of 0.160 ± 0.001 ms for peptide YEQ2Q3, and yet peptide YEQ2Q3 induces ~1.9% larger blockade current amplitude than peptide Q3YEQ2. The obtained results show the remarkable potential of aerolysin nanopores for peptide/protein identification, characterization, sequencing and also demonstrate that the mass identification of nonuniformly charged peptides/proteins by using the nanopore technique could be complicated by their folded structure and complex analyte-pore interaction.

Introduction

Nanopore-based resistive pulse sensing is a highly sensitive single-molecule technology for the detection and analysis of various chemical compounds and biomolecules,[1–7] such as DNA,[8–13] RNA,[14,15] poly(ethylene glycol) (PEG),[16] peptides,[17–23] and proteins.[24–26] This approach is based on the continuous measurement of channel ion current induced by an applied external electric field. When a single molecule passes through the nanopore, a unique current blockage can be observed due to the occupied volume of the pore lumen caused by the molecule.[27,28] The physical and chemical properties of the studied analyte including its size, concentration, conformation, structure, charge, and interaction with the pore can be inferred from statistical analysis of the blockade events.[29–31]

The detection of peptides/proteins by the nanopore technique has become a research hotspot in recent years. Peptides or proteins are basic substances that make up cells, and play important roles in all aspects of life. Many proteins produced in a cell need to traverse through nanopores inserted into membranes to perform specific biological functions.[32] The translocation of proteins into mitochondria,[33,34,36] chloroplasts,[35] endoplasmic reticulum,[45] and nuclear envelope of eukaryotic cells involves complex protein-protein and protein-pore interactions.[37,38] By studying the physical properties and molecular action mechanisms of peptides/proteins with nanopore techniques,[44] more details about the function and dynamics of these crucial biological processes are available.[45–48] There are millions of protein variants in the human proteome, and disease-related variants often appear in minimal concentrations.[39–41] Unlike some traditional detection techniques that rely on ensemble averaging, such as circular dichroism spectra (CD), nuclear magnetic resonance (NMR), and mass spectrometry (MS), nanopore sensors show stronger detection ability in that they can detect a subset of very rare protein events within a larger population,[41,42] and reveal the presence of intermediate conformations.[17,27,43] This portable, low-cost, real-time, label-free nanopore technology has become a powerful tool for diagnostics and therapeutics.[50–52] It provides us with a stochastic, dynamic perspective, which creates infinite possibilities for peptides/proteins sensing and characterization.[49,53–54] Typically, a crucial step towards the developing of nanopore sensing for proteomics is to identify the mass and primary structure of individual peptides/proteins. The previous application of nanopore mass spectrometry in the study of PEG molecules makes the nanopore platform a

[a] F. Hu, S. Li, Prof. A. Zou
Shanghai Key Laboratory of Functional Materials Chemistry
State Key Laboratory of Bioreactor Engineering and Institute of Applied Chemistry
School of Chemistry and Molecular Engineering
East China University of Science and Technology
Shanghai 200237 (P. R. China)
E-mail: aihuazou@ecust.edu.cn
[b] Dr. B. Angelov
Institute of Physics, ELI Beamlines
Academy of Sciences of the Czech Republic
Na Slovance 2, 18221 Prague (Czech Republic)
[c] Dr. N. Li
National Center for Protein Science in Shanghai
Zhangjiang Lab, Shanghai Advanced Research Institute, CAS
Shanghai 200120 (P. R. China)
[d] Dr. X. Lin
Institute of Single Cell Engineering
Beijing Advanced Innovation Center for Biomedical Engineering
Beihang University
Beijing 100191 (P. R. China)
E-mail: linxbseu@buaa.edu.cn

🖥 Supporting information for this article is available on the WWW under https://doi.org/10.1002/cbic.202000119

ChemBioChem

Full Papers
doi.org/10.1002/cbic.202000119

Chemistry Europe
European Chemical
Societies Publishing

potentially ideal tool for use as peptides/proteins mass identifier.[55,56] Many researchers attempted to evaluate the correlation between the current blockade amplitude and the mass of peptide or protein in nanopore experiment, several remarkable results have been achieved.[53,57,58]

Compared with uniformly charged linear ssDNA, peptides/proteins have more complex structures and charge distributions, with various polar and hydrophobic and positively and negatively charged side chains.[48] In addition, peptides and proteins are folded polymers that may exhibit different conformational substates in single-channel detection system, overcomplicating the interpretation of the induced current blockade events across the nanopore.[44,48] Previous work revealed that it is an excellent choice to design model molecules for a preliminary study to simplify the complexity.[17,18,30,59–62]

Recently, Long's group studied the capture and translocation behavior of two series of model peptides (YEQ)$_n$ ($n = 2$, 3, 4) and (YKQ)$_3$ with different charges and lengths using an aerolysin nanopore. The electrostatic effect and length play important roles in the interactions between the peptide and aerolysin interface.[59] This anion-selective aerolysin nanopore has no vestibule but has a long pore lumen (~ 10 nm) with a diameter of 1.0–1.7 nm.[63] One striking feature of aerolysin is that there are various positively and negatively charged residues distributed in its pore lumen (R288, D209, R282, D216, R220, D222, E237, K238, E258, K242, E254, K246, E252, K244).[78] The two main sensing regions of aerolysin nanopore that containing two critical positively charged amino acids of R220 and K238, respectively, were identified by combining the mutant nanopore experiments and molecular dynamics (MD) simulations.[64,79] The aerolysin-analyte interactions at these sensing regions can augment the sensitivity of the targeted analyte readout. Here, taking advantage of the high sensitivity of the aerolysin nanopore,[62] we sought to identify even more similar analytes. We designed two model peptides YEQYEQQDDDRQQQ (YEQ2Q3) and QDDDRQQQYEQYEQ (Q3YEQ2). Even though both peptides have the same amino acid composition, the influence of their amino acid sequence on their intramolecular interactions and therefore the structure is notable, which was demonstrated by all-atom MD simulations. The two similar but differently folded peptides could be identified as they traverse the aerolysin nanopore based on their distinct current blockades. However, the mass-independent current blockades depth indicated that the mass identification of non-uniformly charged peptides/proteins by nanopores may be complicated by their folded structure and complex analyte-pore interaction. Further, voltage-dependent studies were conducted to discuss the energy barrier for the entrance and translocation of these two peptides. Three parameters were used in this work: I/I_0, which is defined as a ratio between the mean blockage residual current during the transit of the analyte across the nanopore (I) and the mean open pore current (I_0); the dwell time, which reflects the elapsed time for a single molecule spends in the nanopore; the frequency, or capture rate, is usually expressed as the number of blockades per second.[49,65] Our efforts will help to obtain an original picture of how two

folded peptides of the same composition traverse the aerolysin nanopore. Together with recent attempts of aerolysin to identify single amino acid,[2–5] our results anticipate that the aerolysin could direct and high-throughput peptides/proteins identification, characterization, potentially sequencing.

Results and Discussion

Based on previous research,[59] the motif (YEQ)$_2$ was introduced to the current design of model peptides. Considering that amino acids E and Y are negatively charged and polar respectively, the motif QDDDRQQQ, rich in negatively charged D and polar Q, was used to design two model peptides with the same amino acid composition but different sequences: YEQYEQQDDDRQQQ (YEQ2Q3) and QDDDRQQQYEQYEQ (Q3YEQ2), which were supposed to have significantly different intramolecular interactions and thus different structures. Properties of the peptides were shown in Figure 2d and Table S1 in the Supporting Information.

As illustrated in Figure 1a, a single wild-type aerolysin nanopore was inserted in a lipid bilayer by self-assembly, separating the *cis* and *trans* compartments filled with an electrolyte solution. With the *cis* side grounded, the negatively charged YEQ2Q3 or Q3YEQ2 can be driven toward and through the aerolysin pore with a positive voltage applied across the membrane. The typical signals for YEQ2Q3 and Q3YEQ2 with the same molecular weight and net charge exhibited significant differences in dwell time (Figure 1b). In particular, at a voltage of $+60$ mV, the statistical dwell times were 0.160 ± 0.001 ms and 0.630 ± 0.018 ms for YEQ2Q3 and Q3YEQ2, respectively. The translocation for Q3YEQ2 in wild-type aerolysin nanopore was four times longer than that for YEQ2Q3; this revealed the existence of a strong interaction between Q3YEQ2 and aerolysin.[59]

Two 100-ns all-atom MD simulations of YEQ2Q3 and Q3YEQ2 with the same initial secondary structure in water solution (Figure S5) were performed. As shown in Figure 2a, structures of peptide YEQ2Q3 and Q3YEQ2 are dramatically different as expected. Compared with Q3YEQ2, YEQ2Q3 has fewer hydrogen bonds and is much more extended, which are further validated by time-evolution analysis of the number of hydrogen bonds (N_{HB}, Figure 2b) and the distance between peptide N/C termini (D_{NC}, Figure 2c). Hydrogen bonds were counted by using GROMACS tool (*gmx hbond*)[82] with the default angle and distance cutoff for proteins. Respectively, YEQ2Q3 and Q3YEQ2 have about 4.40 and 9.60 hydrogen bonds (Figure 2d). Our all-atom MD simulations clearly validated the much stronger hydrogen bonding in Q3YEQ2 than that in YEQ2Q3. Hydrogen bonding, often described as an electrostatic dipole-dipole interaction, is one of the significant driving forces in protein folding,[66] contributes to the formation of a respectively distinct conformation of peptides/proteins.[67] As mentioned, negatively charged amino acids D and E are much closer to each other in the sequence of YEQ2Q3. It is this electrostatic repulsion interaction that drives the formation of the stretched and extended state with fewer hydrogen bonds
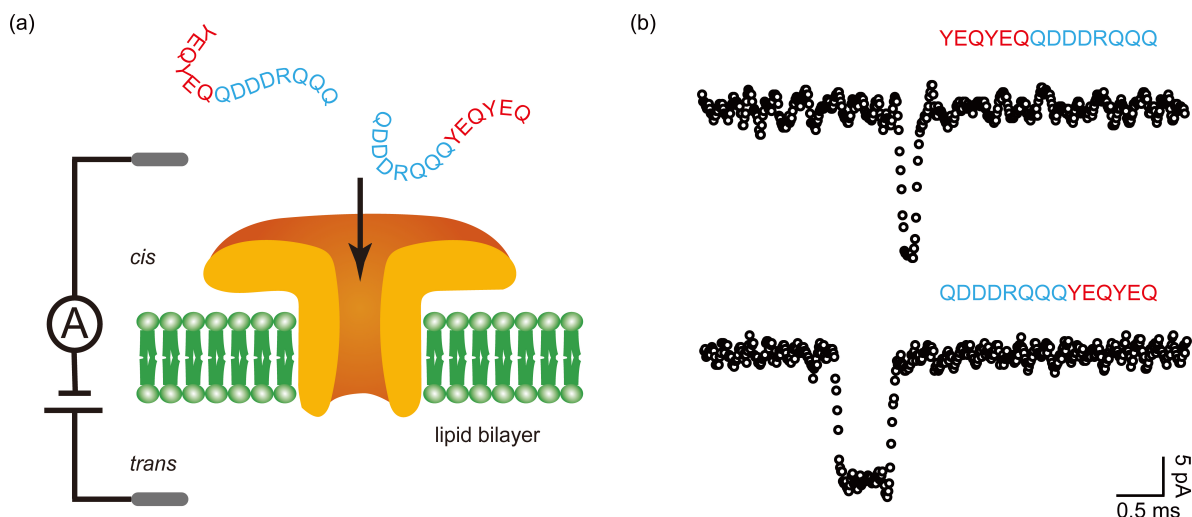
ChemBioChem

Full Papers
doi.org/10.1002/cbic.202000119

Chemistry Europe
European Chemical
Societies Publishing

Figure 1. a) Schematic illustration of the model peptides YEQYEQQDDDRQQQ (YEQ2Q3) and QDDDRQQQYEQYEQ (Q3YEQ2) detected by using a wild-type aerolysin nanopore. The potential across the bilayer is applied by Ag/AgCl electrodes. b) Typical signals for the addition of YEQ2Q3 (top) and Q3YEQ2 (bottom) to the *cis* side of the wild-type aerolysin nanopore. All data were acquired at $+60$ mV, 1.0 M KCl, 10 mM Tris, and 1.0 mM EDTA at pH 8.0. The concentration of each peptide in the *cis* chamber is 30 μM.

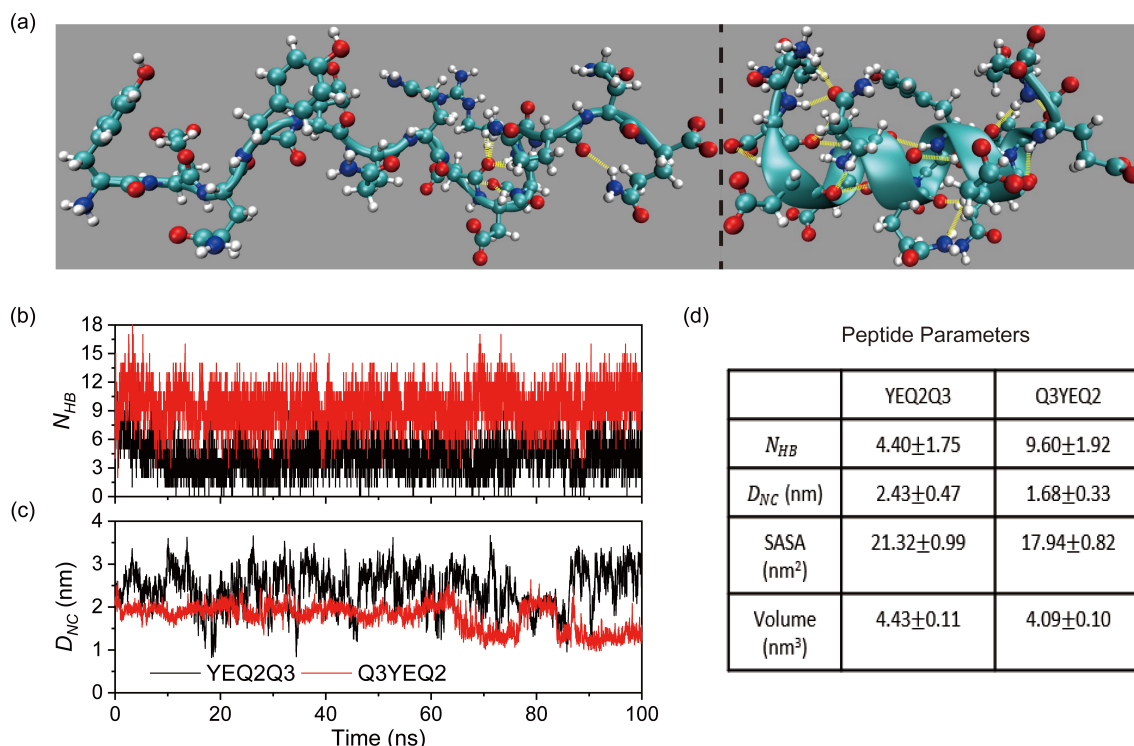|	YEQ2Q3	Q3YEQ2
N_{HB}	4.40 ± 1.75	9.60 ± 1.92
D_{NC} (nm)	2.43 ± 0.47	1.68 ± 0.33
SASA (nm²)	21.32 ± 0.99	17.94 ± 0.82
Volume (nm³)	4.43 ± 0.11	4.09 ± 0.10

Figure 2. a) Representative conformations of peptides YEQ2Q3 (left) and Q3YEQ2 (right) in 100 ns MD simulations. Peptides are shown in ball-and-stick models with the backbone as a carton: C (cyan), N (blue), O (red), H (white). Hydrogen bonds are shown as yellow dashed lines. Time evolution of b) the number of intramolecular hydrogen bonds and c) distance between the N and C termini for the two peptides. d) Peptide parameters (mean $\pm$ sd) were obtained based on the statistics over the last 60 ns of MD simulations.

as stable structure for YEQ2Q3. Similarly, stable and strong hydrogen bonding in Q3YEQ2 maintains its helical structure. In short, the intramolecular hydrogen bonding plays an important role in determining the final structural differences of the two peptides (YEQ2Q3: extended and flexible; Q3YEQ2: compacted and stable; Figure 2a, c), which would bring about different translocation dynamics across the aerolysin channel. On the other hand, by using GROMACS tool (*gmx sasa*)[82], both solvent accessible surface area (SASA) and volume are further calculated (Figure 2d).

These are not the final page numbers! ↗↗

ChemBioChem

Full Papers
doi.org/10.1002/cbic.202000119

Chemistry
Europe
European Chemical
Societies Publishing

To further characterize the peptide blockade, the magnitude of the ionic current associated with a peptide blockade I was normalized to I_0 to mitigate slight fluctuations in I_0 during an experiment.[49] Under an applied voltage of $+60$ mV, the residual current ratio I/I_0 for peptide YEQ2Q3 was centered at 0.320 ± 0.001, whereas peptide Q3YEQ2 displayed a centralized peak at 0.333 ± 0.004 (Figures S1 and S3). The depth of current blockade is related to the volume excluded by the peptide inside the nanopore.[58] The discrepancy in the occupied volume of two peptides inside the nanopore was reflected in that peptide YEQ2Q3 induced $\sim1.9\%$ larger blockade current amplitude than peptide Q3YEQ2, which reveals the high resolution of aerolysin nanopore. However, there would be a deviation between the current signal obtained from the nanopore experiment and the expectation from the peptide mass if we try to use the nanopore as a peptide mass identifier. In our experiment, the two model peptides of the same molecular weight caused distinct mass-independent current blockades (Figure 3a). The lost connection between current blockades depth and mass of peptide is due in part to the fact that these two peptides with non-uniform electrical charge distribution are folded differently, and they can interact complexly with the highly charged pore lumen when confined to the single-molecule sensing interface of aerolysin nanopore. As proposed by Huang and co-workers,[58] the electrostatic interaction between peptide and nanopore can regulate the temporal-spatial resolution required for single-molecule analysis. Nonetheless, it might hinder the accuracy of mass identification. It's also worth mentioning that for both peptides, peptide-induced current blockades showed an explicit dependence on the applied voltage (Figure 3a). One possible reason is that the two peptides undergo dynamic conformational changes at different voltages, as shown in previous paper.[59]

In general, the translocation process for the two peptides are mainly governed by the extended electric field outside the nanopore entrance, the electroosmotic flow (EOF), the entropic barrier associated with peptide conformation,[68,69] the peptide-pore interactions at the aerolysin pore *cis* entrance and aerolysin pore lumen.[5] Both peptides are negatively charged, suggests that electrophoretic forcing is the main driving force. The electro-osmotic flow (EOF), which may also contribute to the driving force, is in the same direction as the peptide translocation (*cis*-to-*trans*) at positive voltage.[2,77] As mentioned above, the two peptides possess entirely different conformations. The volume and surface area of peptide YEQ2Q3 with extended side chains are larger than that of peptide Q3YEQ2 (Figure 2d). In other words, the translocation of peptide YEQ2Q3 through the aerolysin channel needs to overcome more desolvation free energy. Electrostatic effect is also of crucial importance in the interactions between peptide and aerolysin interface.[59,65,79] The attractive electrostatic interactions manifested between the negatively charged peptide and the positively charged amino acids clustered around the *cis* entrance (such as R220, R282 and R288) were expected to facilitate the entrance of the peptide into the pore.[59,78] Similarly, seven unpaired positively charged amino acids located in the inner surface of aerolysin nanopore.[70] Peptide-pore lumen electrostatic interactions reduced the free energy in the initial stage for translocation process, but then contributed to additional energy barrier during the peptide released forward to the *trans* side.[69]

As shown in Figure 4, after adding the peptide Q3YEQ2 into the *cis* side of the aerolysin nanopore, larger amounts of blockades can be observed at voltages of $+100$ and $+140$ mV. To better understand the capture process of the two peptides, we statistically analyzed the event frequency changes with applied voltage (Figure 4c). Peptide Q3YEQ2 was more likely to enter the aerolysin nanopore than peptide YEQ2Q3 over the whole voltage range ($+60$ to $+160$ mV).

Once a peptide is captured by the aerolysin nanopore and induces an electrochemical signal, we need to conduct further voltage-dependent study with dwell time to determine whether this is a successful translocation event.[71] The dwell time of peptide YEQ2Q3 depends nonmonotonically on the applied
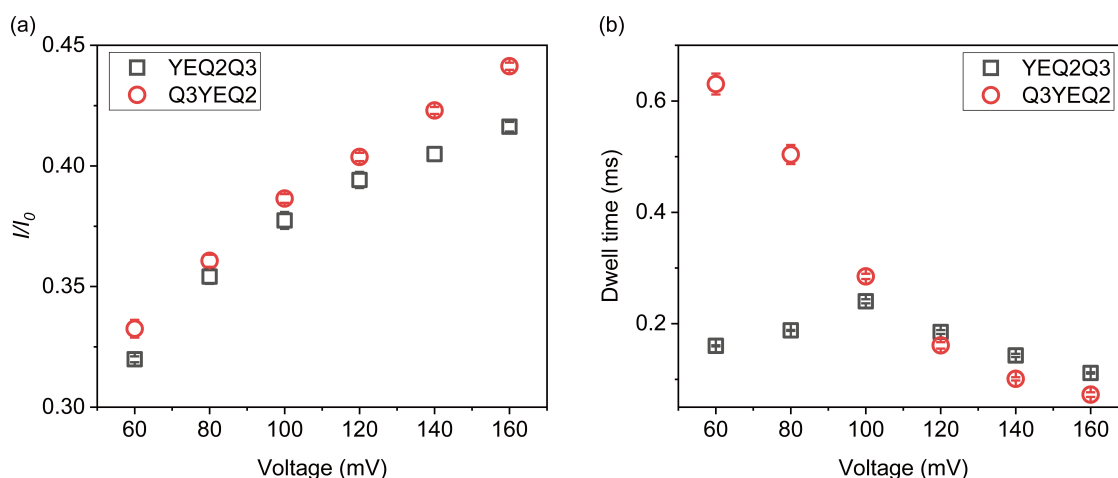

Figure 3. Effects of applied voltage. a) I/I_0 and b) duration for YEQ2Q3 and Q3YEQ2 as a function of applied voltage. Error bars are based on three independent nanopore experiments.
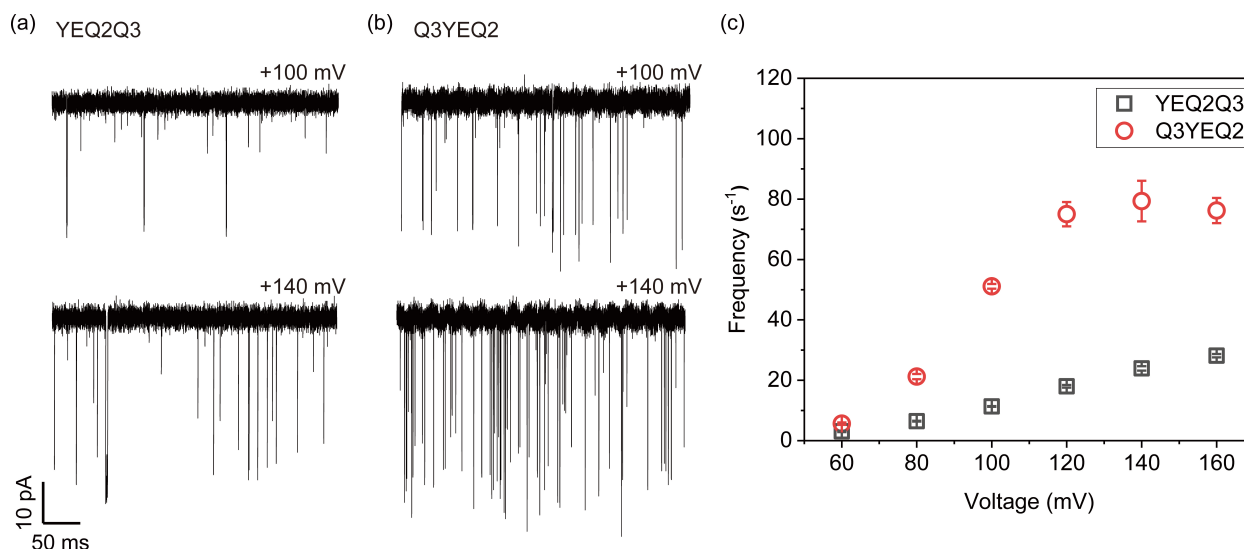
These are not the final page numbers! ↗↗

Figure 4. Raw current recording traces measured after the addition of a) YEQ2Q3 and b) Q3YEQ2 to the *cis* side of the wild-type aerolysin nanopore at $+100$ and $+140$ mV. c) Voltage dependence of the frequency of YEQ2Q3 and Q3YEQ2 by the wild-type aerolysin. The frequency for each peptide captured by the aerolysin pore was calculated from $f = 1/\tau_{on}$, where τ_{on} is the mean interevent interval; the values of τ_{on} for each peptide were determined by single exponential fittings. The error bar is based on three independent nanopore experiments.

voltage, as illustrated in Figure 3b (black squares). Below a threshold voltage of $+100$ mV, the dwell time increased with the transmembrane potential. Peptide YEQ2Q3 simply remained inside the nanopore for a while and then returned back to the initial *cis* compartment. The driving force increased with the voltage magnitude can only keep peptide YEQ2Q3 inside the pore for a longer time, but it was not able to overcome the high-energy barrier set by the aerolysin nanopore for peptide YEQ2Q3 to translocate. By increasing the applied voltage ($> +$ 100 mV), peptide YEQ2Q3 eventually overcame the energy barrier and successfully threaded through the nanopore due to the enhanced electric driving force.[18,71,77] In comparison with YEQ2Q3, peptide Q3YEQ2 shows a monotonic dependence of dwell time on the applied voltage. Peptide Q3YEQ2 can traverse through the nanopore over the whole voltage range ($+60$ to $+160$ mV); a higher energy barrier for YEQ2Q3 entering into the aerolysin can be speculated.[75,76]

For the successful translocation of YEQ2Q3 above $+100$ mV, the relationship between the dwell time of peptide YEQ2Q3 and the applied potential can be scaled as $\tau = \tau_D \exp(-z_{inside}eV/k_BT)$, where τ is the dwell time of YEQ2Q3 traversing through aerolysin, τ_D is a diffusive relaxation time associated with the analyte, e is the magnitude of the elementary charge, k_B is the Boltzmann constant, T is the temperature, and V is the applied potential.[46,65,74,76] We estimated the number of effective charges per YEQ2Q3 inside the aerolysin pore (z_{inside}) and the critical potential (V_c) to be 3.2×10^{-1} and 78 mV, where V_c for YEQ2Q3 is the potential required to overcome the energy barrier traversing inside a confined aerolysin pore, which can be calculated using $V_c = k_BT/z_{inside}e$. Similarly, for peptide Q3YEQ2, the larger z_{inside} value of 5.9×10^{-1} reveals a stronger interaction between Q3YEQ2 and the aerolysin interface compared with YEQ2Q3. There is lower energy barrier for Q3YEQ2 to trans-

locate, the critical potential (V_c) for its translocation is 43 mV which is about 45% lower than YEQ2Q3.

Conclusion

In summary, two model peptides, YEQ2Q3 and Q3YEQ2, with the same amino acid composition but different sequences were investigated by using an aerolysin nanopore. All-atom molecular dynamics (MD) simulations revealed that for the two peptides, the relative distances between negatively charged amino acids D and E and between polar amino acids Q and Y are different. Due to the electrostatic repulsion interaction between negatively charged amino acids D and E, peptide YEQ2Q3 forms a stretched and extended conformation with less hydrogen bonding. Peptide Q3YEQ2 possesses more stable hydrogen bonds and maintains its helical structure. Both peptides induced characteristic electrochemical signals during their translocation process that contained fundamental information about the peptide size, secondary structure, amino acid sequence, etc.[44] We statistically analyzed the translocation dynamic of these two peptides inside the aerolysin and discussed the energy barrier for their entrance and translocation. The two peptides folded differently and exhibited distinct translocation behaviors. Folding is of great importance in detecting peptides/proteins with nanopores.[25,26,42] Many diseases, such as Alzheimer's, mad cow (BSE), and Parkinson's disease, are caused by mutations in important proteins in some cells that cause them to accumulate or misfold. Therefore, an in-depth understanding of the relationship between protein folding and misfolding will be of great help in elucidating the pathogenesis of these diseases and in the search for a cure.[72,73] Aerolysin nanopores, which can identify peptides that are

These are not the final page numbers! ↗↗

ChemBioChem

Full Papers
doi.org/10.1002/cbic.202000119

Chemistry Europe
European Chemical
Societies Publishing

similar but fold differently, is a highly sensitive sensor with great potential in peptides/proteins identification, characterization, and sequencing.

However, the exact relationship between the mass of peptide or protein and the blockade current amplitude is still ambiguous. When studying peptides/proteins with nonuniform charge distribution, the folding and the interaction with nanopores will complicate the mass analysis and sequencing. How to rationally design the single-molecule-sensing interfaces of nanopores (e.g., by site-directed mutagenesis), chemically modify peptides/proteins, or change the solution conditions (e.g., pH, ionic strength) to directly identify the mass of peptides/proteins from the depth of ionic current blockades, further, to successfully recognize blockades induced by individual amino acid, there is still a long way to go.[6,30,53,57,58]

Experimental Section

Reagents and chemicals: The nanopore detection method was the same as that used in previous studies.[79] Trypsin-EDTA and decane (anhydrous, ≥99%) were purchased from Sigma-Aldrich. Diphytanoylsn-glycero-3-phosphocholine (powder, ≥99%) was purchased from Avanti Polar Lipids. Both peptide samples (YE-QYEQQDDDRQQQ; QDDDRQQQYEQYEQ) were synthesized and HPLC-purified by GL Biochem Ltd. (Shanghai, P. R. China). All reagents and materials were of analytical grade. All solutions were prepared using ultrapure water (18.2 MΩ cm at 25 °C) from a Milli-Q system.

Single-channel recording experiments: A single wild-type aerolysin nanopore was inserted into a lipid bilayer formed across a 50 μm diameter horizontal orifice in a Delrin bilayer cup, which separated the aperture into a *cis* chamber and *trans* chamber. All experiments were performed at a temperature of 21±1 °C in 1.0 M KCl, 10 mM Tris, 1.0 mM EDTA, pH 8.0. All peptides were added to the *cis* side of the pore with a final concentration of 30 μM. The current recordings were performed with a patch clamp amplifier (Axon 200B) equipped with a Digidata 1440A A/D converter, Molecular Devices, USA). The signals were low-pass filtered at 5 kHz and acquired with Clampex 10.4 software (Molecular Devices, USA) at a sampling rate of 100 kHz. The data analysis was performed by using MOSAIC[80,81] software and OriginLab 2018 (Origin-Lab, Northampton, MA). The error represents the standard deviation for three independent nanopore experiments.

Molecular modeling and simulations: CHARMM-GUI[83] was used to construct initial structures of YEQ2Q3 and Q3YEQ2, which has the same secondary structure. The peptides were separately solvated in water box (~5 nm×5 nm×5 nm) with 1.0 M KCl. All all-atom MD simulations were performed by using GROAMCS software (version 2016.5)[82] and CHARMM36m force field.[84] For all simulations, the Lennard-Jones potential was smoothly shifted to 0 between 1.0 and 1.2 nm, with a cutoff of 1.2 nm to reduce cutoff noise. Particle mesh Ewald electrostatics[85] with a real-space cutoff of 1.2 nm was used. Peptide and water and ions were coupled separately to Nose-Hoover heat baths[86,87] at $T = 295$ K (coupling constant $t = 1$ ps). The systems were simulated at 1 bar pressure using a Parrinello-Rahman pressure coupling scheme[88] with a coupling constant $t = 5$ ps and compressibility of 4.5×10^{-5} bar^{-1}. Bonds with H-atoms were constrained with the LINCS algorithm.[89] The nonbonded interaction neighbor list was updated every 20 steps with a cutoff of 1.2 nm. Besides, leap-frog Verlet algorithm and periodic boundary conditions were used. All simulations were run for 100 ns with a time step of 2 fs and a trajectory-saving frequency of 10 ps.

## Conflict of Interest

The authors declare no conflict of interest.

[1] M. Chinappi, F. Cecconi, *J. Phys. Condens. Matter* **2018**, *30*, 204002.
[2] B. Yuan, S. Li, Y. L. Ying, Y. T. Long, *Analyst* **2020**, *145*, 1179–1183.
[3] Y. Lu, X. Y. Wu, Y. L. Ying, Y. T. Long, *Chem. Commun.* **2019**, *55*, 9311–9314.
[4] F. N. Meng, Y. L. Ying, J. Yang, Y. T. Long, *Anal. Chem.* **2019**, *91*, 9910–9915.
[5] Y. L. Ying, J. Yang, F. N. Meng, S. Li, M. Y. Li, Y. T. Long, *Research* **2019**, *2019*, 1050735.
[6] Y. L. Ying, Y. T. Long, *J. Am. Chem. Soc.* **2019**, *141*, 15720–15729.
[7] S. Howorka, Z. Siwy, *Chem. Soc. Rev.* **2009**, *38*, 2360–2384.
[8] P. B. Stranges, M. Palla, S. Kalachikov, J. Nivala, *Proc. Natl. Acad. Sci. USA* **2016**, *113*, 6749–6756.
[9] J. J. Kasianowicz, E. Brandin, D. Branton, D. W. Deamer, *Proc. Natl. Acad. Sci. USA* **1996**, *93*, 13770–13773.
[10] J. J. Wang, M. Y. Li, J. Yang, Y. Q. Wang, X. Y. Wu, J. Huang, Y. L. Ying, Y. T. Long, *ACS Cent. Sci.* **2020**, *6*, 76–82.
[11] N. An, A. M. Fleming, H. S. White, C. J. Burrows, *Proc. Natl. Acad. Sci. USA* **2012**, *109*, 11504–11509.
[12] N. Ashkenasy, J. Sánchez-Quesada, H. Bayley, M. R. Ghadiri, *Angew. Chem. Int. Ed. Engl.* **2005**, *44*, 1401–1404.
[13] M. Jain, S. Koren, K. H. Miga, J. Quick, A. C. Rand, T. A. Sasani, J. R. Tyson, A. D. Beggs, A. T. Dilthey, I. T. Fiddes, S. Malla, H. Marriott, T. Nieto, J. O'Grady, H. E. Olsen, B. S. Pedersen, A. Rhie, H. Richardson, A. R. Quinlan, T. P. Snutch, L. Tee, B. Paten, A. M. Phillippy, J. T. Simpson, N. J. Loman, M. Loose, *Nat. Biotechnol.* **2018**, *36*, 338–345.
[14] M. Akeson, D. Branton, J. J. Kasianowicz, E. Brandin, D. W. Deamer, *Biophys. J.* **1999**, *77*, 3227–3233.
[15] Y. Wang, D. Zheng, Q. Tan, M. X. Wang, L. Q. Gu, *Nat. Nanotechnol.* **2011**, *6*, 668–674.
[16] J. W. F. Robertson, C. G. Rodrigues, V. M. Stanford, K. A. Rubinson, O. V. Krasilnikov, J. J. Kasianowicz, *Proc. Natl. Acad. Sci. USA* **2007**, *104*, 8207–8211.
[17] T. C. Sutherland, Y. T. Long, R. I. Stefureac, I. Bediako-Amoa, H. B. Kraatz, J. S. Lee, *Nano Lett.* **2004**, *4*, 1273–1277.
[18] L. Movileanu, J. P. Schmittschmitt, J. M. Scholtz, H. Bayley, *Biophys. J.* **2005**, *89*,1030–1045.
[19] A. Asandei, A. Apetrei, Y. Park, K. S. Hahm, T. Luchian, *Langmuir* **2011**, *27*, 19–24.
[20] L. Mereuta, I. Schiopu, A. Asandei, Y. Park, K. S. Hahm, T. Luchian, *Langmuir* **2012**, *28*, 17079–17091.
[21] A. Asandei, I. Schiopu, S. Ifemi, L. Mereuta, T. Luchian, *Langmuir* **2013**, *29*, 15634–15642.
[22] L. Mereuta, M. Roy, A. Asandei, J. K. Lee, Y. Park, I. Andricioaei, T. Luchian, *Sci. Rep.* **2014**, *4*, 3885.
[23] L. Mereuta, A. Asandei, C. H. Seo, Y. Park, T. Luchian, *ACS Appl. Mater. Interfaces* **2014**, *6*, 13242–13256.
[24] A. Han, M. Creus, G. Schürmann, V. Linder, T. R. Ward, N. F. de Rooij, U. Staufer, *Anal. Chem.* **2008**, *80*, 4651–4658.
[25] G. Oukhaled, J. Mathé, A. L. Biance, L. Bacri, J. M. Betton, D. Lairez, J. Pelta, L. Auvray, *Phys. Rev. Lett.* **2007**, *98*, 158101.
[26] D. S. Talaga, J. Li, *J. Am. Chem. Soc.* **2009**, *131*, 9287–9297.

[27] C. Cao, D. F. Liao, J. Yu, H. Tian, Y. T. Long, *Nat. Protoc.* **2017**, *12*, 1901–1911.

[28] C. Cao, Y. T. Long, *Acc. Chem. Res.* **2018**, *51*, 331–341.

[29] J. W. F. Robertson, J. E. Reiner, *Proteomics* **2018**, *18*, 1800026.

[30] A. Asandei, A. E. Rossini, M. Chinappi, Y. Park, T. Luchian, *Langmuir* **2017**, *33*, 14451–14459.

[31] Y. L. Ying, C. Cao, Y. X. Hu, Y. T. Long, *Natl. Sci. Rev.* **2018**, *5*, 450–452.

[32] A. J. Wolfe, M. M. Mohammad, S. Cheley, H. Bayley, L. Movileanu, *J. Am. Chem. Soc.* **2007**, *129*, 14034–14041.

[33] C. Muro, S. M. Grigoriev, D. Pietkiewicz, K. W. Kinnally, M. L. Campo, *Biophys. J.* **2003**, *84*, 2981–2989.

[34] P. Rehling, K. Model, K. Brandner, P. Kovermann, A. Sickmann, H. E. Meyer, W. Kuhlbrandt, R. Wagner, K. N. Truscott, N. Pfanner, *Science* **2003**, *299*, 1747–1751.

[35] S. C. Hinnah, R. Wagner, N. Sveshnikova, R. Harrer, J. Soll, *Biophys. J.* **2002**, *83*, 899–911.

[36] K. Gabriel, S. K. Buchanan, T. Lithgow, *Trends Biochem. Sci.* **2001**, *26*, 36–40.

[37] S. M. Simon, C. S. Peskin, G. F. Oster, *Proc. Natl. Acad. Sci. USA* **1992**, *89*, 3770–3774.

[38] W. Wickner, R. Schekman, *Science* **2005**, *310*, 1452–1456.

[39] Y. Zhao, B. Ashcroft, P. Zhang, H. Liu, S. Sen, W. Song, J. Im, B. Gyarfas, S. Manna, S. Biswas, C. Borges, S. Lindsay, *Nat. Nanotechnol.* **2014**, *9*, 466–473.

[40] M. Uhlen, F. Ponten, *Mol. Cell. Proteomics* **2005**, *4*, 384–393.

[41] A. I. Archakov, Y. D. Ivanov, A. V. Lisitsa, V. G. Zgoda, *Proteomics* **2007**, *7*, 4–9.

[42] K. J. Freedman, M. Jürgens, A. Prabhu, C. W. Ahn, P. Jemth, J. B. Edel, M. J. Kim, *Anal. Chem.* **2011**, *83*, 5137–5144.

[43] L. Ma, S. L. Cockroft, *ChemBioChem* **2010**, *11*, 25–34.

[44] L. Movileanu, *Soft Matter* **2008**, *4*, 925–931.

[45] T. Hessa, H. Kim, K. Bihlmaier, C. Lundin, J. Boekel, H. Andersson, I. Nilsson, S. H. White, G. von Heijne, *Nature* **2005**, *433*, 377–381.

[46] A. Oukhaled, L. Bacri, M. Pastoriza-Gallego, J. M. Betton, J. Pelta, *ACS Chem. Biol.* **2012**, *7*, 1935–1949.

[47] D. Fologea, B. Ledden, D. S. McNabb, J. Li, *Appl. Phys. Lett.* **2007**, *91*, 539011–539013.

[48] L. Movileanu, *Trends Biotechnol.* **2009**, *27*, 333–341.

[49] N. Varongchayakul, J. Song, A. Meller, M. W. Grinstaff, *Chem. Soc. Rev.* **2018**, *47*, 8512–8524.

[50] J. M. Asara, M. H. Schweitzer, L. M. Freimark, M. Phillips, L. C. Cantley, *Science* **2007**, *316*, 280–285.

[51] O. Tavassoly, J. Kakish, S. Nokhrin, O. Dmitriev, J. S. Lee, *Eur. J. Med. Chem.* **2014**, *88*, 42–54.

[52] S. Wang, F. Haque, P. G. Rychahou, B. M. Evers, P. Guo, *ACS Nano* **2013**, *7*, 9814–9822.

[53] G. Huang, K. Willems, M. Soskine, C. Wloka, G. Maglia, *Nat. Commun.* **2017**, *8*, 935.

[54] N. Shrestha, S. L. Bryant, C. Thomas, D. Richtsmeier, X. Pu, J. Tinker, D. Fologea, *Sci. Rep.* **2017**, *7*, 2448.

[55] J. W. F. Robertson, C. G. Rodrigues, V. M. Stanford, K. A. Rubinson, O. V. Krasilnikov, J. J. Kasianowicz, *Proc. Natl. Acad. Sci. USA* **2007**, *104*, 8207–8211.

[56] M. A. Aksoyoglu, R. Podgornik, S. M. Bezrukov, P. A. Gurnev, M. Muthukumar, V. A. Parsegian, *Proc. Natl. Acad. Sci. USA* **2016**, *113*, 9003–9008.

[57] A. E. Chavis, K. T. Brady, G. A. Hatmaker, C. E. Angevine, N. Kothalawala, A. Dass, J. W. F. Robertson, J. E. Reiner, *ACS Sens.* **2017**, *2*, 1319–1328.

[58] G. Huang, A. Voet, G. Maglia, *Nat. Commun.* **2019**, *10*, 835.

[59] S. Li, C. Cao, J. Yang, Y. T. Long, *ChemElectroChem* **2019**, *6*, 126–129.

[60] R. Stefureac, Y. T. Long, H. B. Kraatz, P. Howard, J. S. Lee, *Biochemistry* **2006**, *45*, 9172–9179.

[61] A. Asandei, M. Chinappi, H. K. Kang, C. H. Seo, L. Mereuta, Y. Park, T. Luchian, *ACS Appl. Mater. Interfaces* **2015**, *7*, 16706–16714.

[62] F. Piguet, H. Ouldali, M. Pastoriza-Gallego, P. Manivet, J. Pelta, A. Oukhaled, *Nat. Commun.* **2018**, *9*, 966.

[63] T. Chakraborty, A. Schmid, S. Notermans, R. Benz, *Infect. Immun.* **1990**, *58*, 2127–2132.

[64] C. Cao, N. Cirauqui, M. J. Marcaida, E. Buglakova, A. Duperrex, A. Radenovic, M. D. Peraro, *Nat. Commun.* **2019**, *10*, 4918.

[65] C. Cao, Y. L. Ying, Z. L. Hu, D. F. Liao, H. Tian, Y. T. Long, *Nat. Nanotechnol.* **2016**, *11*, 713–718.

[66] A. V. Efimov, E. V. Brazhnikov, *FEBS Lett.* **2003**, *554*, 389–393.

[67] F. R. Souza, M. P. Freitas, *Comput. Theor. Chem.* **2011**, *964*, 155–159.

[68] M. Muthukumar, *J. Biomol. Struct. Dyn.* **2013**, *31*, 133–133.

[69] M. Muthukumar, *J. Chem. Phys.* **2003**, *118*, 5174.

[70] M. T. Degiacomi, I. Iacovache, L. Pernot, M. Chami, M. Kudryashev, H. Stahlberg, F. G. van der Goot, M. D. Peraro, *Nat. Chem. Biol.* **2013**, *9*, 623–629.

[71] M. M. Mohammad, L. Movileanu, *Eur. Biophys. J.* **2008**, *37*, 913–925.

[72] C. M. Dobson, *Nature* **2003**, *426*, 884–890.

[73] C. Soto, S. Pritzkow, *Nat. Neurosci.* **2018**, *21*, 1332–1340.

[74] J. Nakane, M. Wiggin, A. Marziali, *Biophys. J.* **2004**, *87*, 615–621.

[75] Z. L. Hu, M. Y. Li, S. C. Liu, Y. L. Ying, Y. T. Long, *Chem. Sci.* **2019**, *10*, 354–358.

[76] J. Yang, Y. Q. Wang, M. Y. Li, Y. L. Ying, Y. T. Long, *Langmuir* **2018**, *34*, 14940–14945.

[77] M. Boukhet, F. Piguet, H. Ouldali, M. Pastoriza-Gallego, J. Pelta, A. Oukhaled, *Nanoscale* **2016**, *8*, 18352–18359.

[78] Y. Wang, L. Q. Gu, K. Tian, *Nanoscale* **2018**, *10*, 13857–13866.

[79] Y. Q. Wang, M. Y. Li, H. Qiu, C. Cao, M. B. Wang, X. Y. Wu, J. Huang, Y. L. Ying, Y. T. Long, *Anal. Chem.* **2018**, *90*, 7790–7794.

[80] A. Balijepalli, J. Ettedgui, A. T. Cornio, J. W. F. Robertson, K. P. Cheung, J. J. Kasianowicz, C. Vaz, *ACS Nano* **2014**, *8*, 1547–1553.

[81] J. H. Forstater, K. Briggs, J. W. Robertson, J. Ettedgui, O. MarieRose, C. Vaz, J. J. Kasianowicz, V. Tabard-Cossa, A. Balijepalli, *Anal. Chem.* **2016**, *88*, 11900–11907.

[82] M. J. Abraham, T. Murtola, R. Schulz, S. Páll, J. C. Smith, B. Hess, E. Lindahl, *SoftwareX* **2015**, *1*, 19–25.

[83] S. Jo, T. Kim, V. G. Iyer, W. Im, *J. Comput. Chem.* **2008**, *29*, 1859–1865.

[84] J. Huang, S. Rauscher, G. Nawrocki, T. Ran, M. Feig, B. L. de Groot, H. Grubmüller, A. D. MacKerell Jr., *Nat. Methods* **2017**, *14*, 71.

[85] U. Essmann, L. Perera, M. L. Berkowitz, T. Darden, H. Lee, L. G. Pedersen, *J. Chem. Phys.* **1995**, *103*, 8577–8593.

[86] W. G. Hoover, *Phys. Rev. A* **1985**, *31*, 1695.

[87] S. Nosé, *Mol. Phys.* **1984**, *52*, 255–268.

[88] M. Parrinello, A. Rahman, *J. Appl. Phys.* **1981**, *52*, 7182–7190.

[89] B. Hess, H. Bekker, H. J. Berendsen, J. G. Fraaije, *J. Comput. Chem.* **1997**, *18*, 1463–1472.

FULL PAPERS

Dwelling pace: Two model peptides YEQYEQQDDDRQQQ and QDDDRQQQYEQYEQ were investigated at the single-molecule level. The relative distances between negatively charged residues D and E and between polar residues Q and Y are different, thus the peptides have different intramolecular interactions and structures. When they enter a single aerolysin nanopore, they induce distinct current blockades with characteristic dwell times.

model peptides
YEQYEQQDDDRQQQ
Aerolysin
QDDDRQQQYEQYEQ
cis   trans
10 pA
1 ms
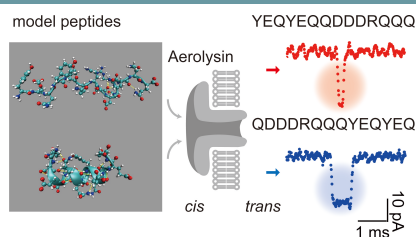
F. Hu, Dr. B. Angelov, S. Li, Dr. N. Li, Dr. X. Lin*, Prof. A. Zou*

1 – 8

Single-Molecule Study of Peptides with the Same Amino Acid Composition but Different Sequences by Using an Aerolysin Nanopore

Single-molecule study of peptides with the same amino acid composition but different sequences by using an aerolysin nanopore (Zou at East China University of Science and Technology)

Share your work on social media! *ChemBioChem* has added Twitter as a means to promote your article. Twitter is an online microblogging service that enables its users to send and read short messages and media, known as tweets. Please check the pre-written tweet in the galley proofs for accuracy. If you, your team, or institution have a Twitter account, please include its handle @username. Please use hashtags only for the most important keywords, such as #catalysis, #nanoparticles, or #proteindesign. The ToC picture and a link to your article will be added automatically, so the **tweet text must not exceed 250 characters**. This tweet will be posted on the journal's Twitter account (follow us @ChemBioChem) upon publication of your article in its final (possibly unpaginated) form. We recommend you to re-tweet it to alert more researchers about your publication, or to point it out to your institution's social media team.

ORCID (Open Researcher and Contributor ID)

Please check that the ORCID identifiers listed below are correct. We encourage all authors to provide an ORCID identifier for each coauthor. ORCID is a registry that provides researchers with a unique digital identifier. Some funding agencies recommend or even require the inclusion of ORCID IDs in all published articles, and authors should consult their funding agency guidelines for details. Registration is easy and free; for further information, see http://orcid.org/.

Dr. Na Li
Fangzhou Hu
Shuang Li
Prof. Aihua Zou http://orcid.org/0000-0002-7672-828X
Dr. Xubo Lin
Dr. Borislav Angelov